Investigation into variation of resistivity and permittivity of aqueous solutions and soils with frequency and current density

Ashwin Desai Belaguppa Manjunath, *Member, IEEE,* Fatima Khan, Nurym Noyanbayev, Noureddine Harid, Huw Griffiths, Ricardo Pereira Nogueira, Nilson Tadeu Camarinho De Oliveira, Manu Haddad, *Member, IEEE,* and Sarathi Ramanujam, *Sr. Member, IEEE*

***Abstract*—Soil parameter characterization and the variation of permittivity and resistivity with frequency (dispersion) and current density has been the subject of many experimental studies but significant differences in measured values are found in the literature due to different testing approaches, apparatus and test sample composition. This paper first presents a comprehensive review of this previous body of work. Then, new experiments on soils and electrolytes with test frequencies in the range 1 Hz to 10 MHz and with current densities from 1 to 35 mA/m^2 are described. Such results help clarify the effects of frequency, soil moisture, electrolyte concentration and electrode material on the measured test medium parameters. The contribution of the electrode-electrolyte interface (EEI) and the influence of current density are particularly highlighted. These findings indicate that some previous measurements may have overestimated the measured values of resistivity and permittivity due to the EEI effect. Finally, the test results are compared with soil parameter equations from CIGRE TB781.**

***Index Terms*—resistivity, electrode-electrolyte interface, soil, permittivity, nonlinearity, grounding**

I. INTRODUCTION

Grounding is an important aspect of power systems from the viewpoint of power system reliability, equipment protection and human safety. Designing a suitable grounding system requires at least a reasonably accurate quantification of soil parameter values; particularly conductivity, σ, (usually expressed as resistivity, ρ, in grounding literature), and for high frequency (transients) the relative permittivity, ε_r. For most soils, relative magnetic permeability can be assumed to be unity [1]. The variation of resistivity and permittivity of soils (and electrolytes) with frequency, also known as dispersion, and with current-density has been studied by several investigators over many years [2]–[20]. Lightning currents cover a wide range of magnitudes (~1 kA - 300 kA) [21] and frequency components up to 2MHz [22] or 10MHz [23]. Power system ground return fault currents can reach magnitudes of several tens of kA [24]. Therefore, the effect of frequency and current magnitude on ground impedance over these ranges should be accounted for in grounding system design. Practical verification of grounding installations is commonly achieved by measuring ground resistance or ground impedance using low voltage AC or switched DC test equipment. Such equipment may inject only a few amperes of current into the grounding system, sometimes in the order of mA, which represents a small fraction of the actual current that may flow under fault conditions. IEEE standards [25], [26] recognize the effect of current magnitude on soil resistivity and grounding impedance in terms of thermal effects at high current, causing drying out and soil ionization; however, no reference is made to the non-linear characteristics of resistivity (or permittivity) and electrode impedance over a low magnitude current range as will be shown later in this study.

Soil is a nonhomogeneous material; it contains solid particles, voids, and different inorganic salts that behave as electrolytes. If a portion of soil is energized with the introduction of two metallic electrodes to form a closed electric circuit, both conductive and displacement currents will flow. The magnitudes and relative proportions of these constituent currents depend on a multitude of factors including the type of soil, soil structure (porosity), moisture level, temperature, pressure, composition and concentration of dissolved salts as well as the type and amplitude of the applied energization. Accordingly, these physical factors determine the measured values of the bulk electrical parameters (σ and ε) of the soil. Accurate measurement of these bulk parameters is challenging, as the measuring technique and test system, whether in the laboratory or the field, can affect significantly their values. In particular, the interface formed between the metallic electrodes and the soil (electrode-electrolyte interface - EEI)) can significantly affect the measured values [27].

Presenting first a clarification of soil parameter terminologies, this paper then provides a comprehensive review of the findings of previous experimental work focusing on the frequency range 1 Hz to 10^7 Hz and test current magnitudes between 3 mA and 4000 mA. Nonlinearities outside this range of frequencies, and those which occur at much higher current densities due to soil ionization have been studied elsewhere and lie outside the scope of the present investigation.

Following this, the results of a systematic experimental study on soils of controlled moisture content and electrolytic solutions of different ionic concentration are presented. The

Manuscript received x x 2020; revised x x, 2020; accepted x x, 2020. Date of publication x x 2020; date of current version x x 2020. This work was supported by the APEC research center at Khalifa University. Ashwin Manjunath, Fatima Khan, Nurym Noyanbayev, Noureddine Harid, Ricardo Nogueira and Nilson De Oliveira are with Khalifa University, Abu Dhabi 127788, UAE (e-mail: ashwin.manjunath@ku.ac.ae, fatima.khan@ku.ac.ae, nurym.noyanbayev@ku.ac.ae, noureddine.harid@ku.ac.ae, ricardo.nogueira@ku.ac.ae, nilson.deoliveira@ku.ac.ae). Huw Griffiths and Manu Haddad are with Cardiff University, Cardiff, Wales (e-mail: Griffithsh@cf.ac.uk,haddad@cf.ac.uk). Sarathi Ramanujam is with IIT Madras, Chennai, 630036, India (e-mail: rsarathi@ee.iitm.ac.in)

conduction in wet soils is predominantly electrolytic rather than through the solid earth material [12], [28]. Also, the polarization and consequently displacement current is predominantly controlled by the interfaces formed between the soil material and the electrolyte. Therefore, the first step in characterizing the soil electrical parameters' variation is to understand the response of electrolytes when subjected to electric field. By gaining a better understanding of the dispersion of the parameters of the aqueous solutions, the observed dispersion in soil electrical parameters can be explained and predicted. Single salt electrolytic solutions were used as benchmarks for the subsequent soil studies because (i) it ensures consistent and intimate contact between the test medium and the electrodes and (ii) the EEI effect can be more readily discriminated from bulk behavior. Finally, the experimental results are compared with equations from CIGRE TB781 [29].

II. DEFINITIONS AND TERMINOLOGIES OF SOIL PARAMETERS

The relationship between current density and applied electric field in a medium can be expressed by (1) and a derivation and explanation of terms is given in Appendix I.

$$\widetilde{J_t} = \left[\sigma_{eff} + j\omega\epsilon_{r(eff)}\epsilon_0\right]\widetilde{E} \quad (1)$$

where, $$\sigma_{eff} = \sigma' - \omega\epsilon_r''\epsilon_0 \quad (2)$$

and $$\epsilon_{r(eff)} = \frac{\sigma''}{\omega\epsilon_0} + \epsilon_r' \quad (3)$$

Recognizing that different qualifying terms of conductivity and permittivity appear in the literature, the terms effective conductivity (σ_{eff}) and effective relative permittivity ($\varepsilon_{r(eff)}$) in this paper are intended to signify that the values represent the macroscopic properties of the test medium and applicable in the case of soil which contains a multitude of components. The terms 'apparent conductivity' and 'apparent relative permittivity' are common when quantities are obtained from direct measurement of impedance. However and as clarified in this paper, such measured quantities are not necessarily true bulk parameters of the test medium because they include the influence of electrode-electrolyte interface (EEI) comprising the Stern and the Gouy-Chapman layers [20], [30] and where the extent of such influence depends on the type of measurement setup, temperature, the constituent test materials and energization magnitude and frequency. Finally, it is noted that such soil parameters can be derived from impedance measurements based on assuming either a series [31] or parallel [32], equivalent circuit model (of resistance and capacitance). The experimental data presented in this paper are described as apparent values based on a parallel model assumption and resistivity is shown instead of conductivity.

III. REVIEW OF LABORATORY AND FIELD TEST APPROACHES

A large number of investigations have been carried out to measure soil/electrolyte parameters in the laboratory [2]–[5], [7], [10], [15], [16], [33]–[43] while some tests were done in the field [44], [45] . Details of the test medium, test apparatus, arrangements and energizations used in these investigations are described. Before presenting a detailed comparative analysis of the measurement results, some general observations are made about test cells, samples, measurement techniques, and the electrode materials that were previously used.

A. Laboratory measurements

1) Topologies of test cells and electrode arrangements

With reference to Table I, various shapes of test cells have been used including cylindrical (C), hemispherical (H) and cuboidal (Cub). Depending on the selection of electrode terminals, the current path in the test medium may be longitudinal (L), radial (R) or non-uniform. The path length between the current injection electrodes ranged from hundreds of micrometers to 1m. Where current flow is non-uniform resulting in varying current density through the test sample, the determined values of the test medium parameters will be approximate and will not account for current density dependence. The length to area ratio of the test cell was minimized to reduce fringing effects in [3], [8], [18], while others have used a guard ring arrangement to avoid the influence of such effects [35], [37].

2) Electrode materials

Various current injection electrode materials have been used including brass and copper [2], [46], while some [3], [47] coated the test samples with silver paint and gold. With the aim of reducing the effect of the EEI on the measurement of sample impedance for two-terminal tests, platinized platinum electrodes with an interface between the electrode and blotting paper soaked in silver/silver chloride suspension were employed [5]. It was found that such an electrode/electrolyte interface arrangement was superior, in terms of minimizing the EEI effect, to others including stainless steel, platinum, silver, silver chloride and copper electrodes in conjunction with blotting paper soaked in sodium chloride, silver nitrate or copper sulphate. Other investigators [18] with the same aim, also used platinum sputtered electrodes.

3) Soil samples

A variety of soils were tested including sandstone, limestone, shale, alluvium, and clay. Some investigators took a number of samples from a single site [35] while others have collected a large number of samples from different sites [2], [46]. Some samples were taken from near the surface in open fields [35] while others comprised core sections taken from drill holes [3]. Visacro et al. [44] tested a wide range of soil types in-situ. Datsios and Mikropoulos tested sand samples with different grain sizes [28].

4) Measurement technique

The two-terminal [1]–[3], [18] test setup has been used most frequently while some researchers have used both 2 and 4-terminal arrangements [4], [46], [48] . As shown in Fig. 1a, the two-terminal measurement employs the same single pair of electrodes to inject current through, and to measure voltage across, the test cell. In this case, the impedance of the test sample is determined from the quotient of voltage and current ($Z(\omega)=V(\omega)/I(\omega)$), and it will include that of the bulk medium and the interface (EEI). With the four-terminal measurement, separate pairs of current and voltage electrodes are used (Fig. 1b); with the voltage measurement taken across a section of the

TABLE I
TESTS ARRANGEMENTS FOR MEASUREMENT OF RESISTIVITY AND RELATIVE PERMITTIVITY

Investigator	Lab/ Field	Sample type	Test cell shape and current flow	No. test terminals	Current path length	Electrode material	Measurement system	Frequency range	Supply Voltage	J @ ~ 100 Hz (A/m^2)
Smith-Rose [2]	L	Natural site soil	C/L/R	2	-	Copper, brass	Valve oscillating circuit	100 kHz-10 MHz	0.5 V	-
Keller & Licastro [3]	L	Sandstone/ mudstone	C/L	2	-	Sliver paint and brass	Bridge circuit	50 Hz-30 MHz	-	-
Scott et al. [5]	L	Shale, alluvium, quartz etc.	C/L	2	1.3, 2.5 cm	Platinized platinum, silver	Bridge circuit	100 Hz-1 MHz	-	-
Eberle [16]	L	Quartz sand	C/L	2	-	Platinized platinum	Bridge circuit	100 Hz-100 MHz	-	-
Garrouch & Sharma [4]	L	Shaly sand, sandstone etc.	C/L	2&4	3–10 mm	-	LCR meter impedance analyzer	5 Hz - 10 MHz	-	-
Lesmes & Frye[38]	L	Berea sandstone		2&4	-	Platinum	LCR meter/ DAQ	1 mHz - 1MHz	-	-
Miranda et al. [39]	L	LiCl solutions, distilled water	Cub/L	2	5.25 mm	Stainless steel	Impedance analyzer	1 kHz - 13 MHz	-	-
Montana et al. [42]	L	Sand	H/R	2	-	Copper	Impulse gen/ oscilloscope	1 kHz – 3 MHz	1-6.6 kV	-
He et al. [43]	L	–	C/L	2	-	-	Broadband spectrometer	1 Hz -20 MHz	-	-
Duarte et al. [33]	L	Deionized water	C/L	2	0.5–4 mm	Steel, titanium, gold, platinum	Impedance analyzer	1 mHz – 1 MHz	20 mV	< $2.7\cdot10^{-5}$
Duarte et al. [34]	L	KCl solution, deionized water	C/L	2	4 mm	Titanium	Impedance analyzer	1 mHz – 30 MHz	20 mV	< 0.3
Alipio & Visacro [55]	F	Soil from 31 sites	H/R	3&4	-	-	Impulse generator/ oscilloscope	100 Hz – 4 MHz	0.5 – 2 kV	-
Hasan et al. [35]	L	Soil, 1 site	Cub/L	2	50 mm	Copper	RF generator, oscilloscope	50 Hz – 1 MHz	-	<0.63
Revil et al. [36]	L	Peat, sand, clay	-	4	2 cm	Ag-AgCl	Impedance analyzer	1 Hz – 45 kHz	1 V	-
Datsios et al. [37]	L	Silica sand	Cub/L	2	1.3 - 3.2 cm	Stainless steel	LCR meter	42 Hz – 1 MHz	1 V	< 0.22
Zhou et al. [48]	L	Sandy, Silty and clay soil/loam	Cub/L	2,4	22 cm	Stainless steel, brass	LCR meter	50 Hz-10 200 kHz	-	-
Wang et al. [47]	L	Yellow soil	C/L	2	-	Gold plated	Impedance analyzer	50 Hz-1 MHz	-	-
Datsios and Mikropoulos [28]	L	Sandy soil	Cub/L	2	1.3 - 3.2cm	Stainless steel	LCR meter	42 Hz-1 MHz	1V	<0.22
Kuklin [45]	F	-	-	4	-	-	Lab developed device	10 kHz -4MHz	-	-

test sample so as not to include the EEI contribution. Fig. 1c shows a laboratory setup employing a concentric hemispherical test chamber using the 2-terminal measuring technique. Fig 1.d shows a field test setup, also employing a hemispherical test electrode, using the 4-terminal setup where potential measurements are taken at two points along a straight line on the ground surface.

An alternative inductive test method [49], [50] that eliminates the EEI effect has been proposed which uses two parallel toroidal coils (primary and secondary) placed inside the test medium; an arrangement more suited to testing liquid samples. Another technique [6] proposed to discriminate between EEI and bulk medium impedance by testing the same sample material with different length test cells, although some reservations were made about its accuracy [8]. Nevertheless, the two or four-terminal measurement setups are preferred by most investigators for in-laboratory tests and the latter to discriminate directly between bulk medium and electrode

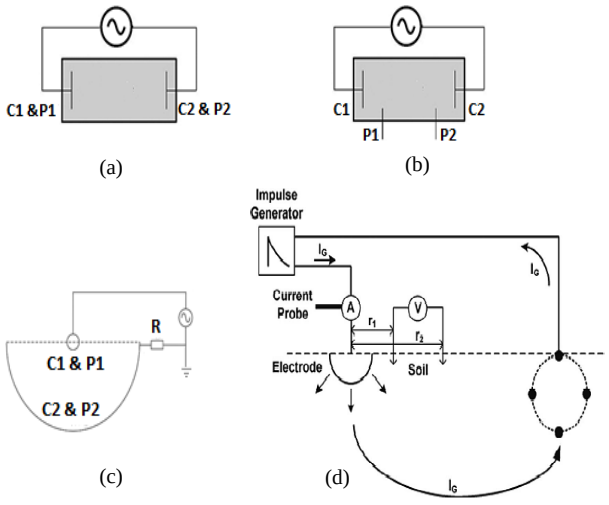

Fig. 1. Adapted examples of test setups: (a) 2-terminal (b) 4-terminal [51], (c) 2-terminal hemispherical [41], (d)4-terminal hemispherical field test [52]

interface impedances [51].

Four-terminal measurements require a very high input impedance at the input terminals of the measuring device to which potential electrodes are connected [4].

5) Test instrumentation and compensation

With reference to Table I, early tests used valve-based oscillators and bridge circuits, while more recently, impedance analyzers, oscilloscopes and LCR meters have been employed. Improvements in measurement accuracy were introduced through test cell calibration to minimize errors due to lead inductance and stray capacitance [8].

B. Field measurements

Wenner and Schlumberger 4-terminal ground surface test methods [26], among others, are employed in the field for soil resistivity measurements using low frequency switched DC energization. Due to parallelism of the current and voltage test leads and the size of test electrodes, such arrangements are normally limited to testing over a narrow low frequency range with low current density. However, electric dipole antennas located in deep vertical boreholes [11] were used to evaluate soil conductivity and permittivity in the frequency range 1 – 10 MHz applying FFT to the measured voltage and current signals. Good agreement was reported between the field tests and laboratory tests of samples taken from the same boreholes. An extensive set of field tests to investigate soil parameter variation over of a wide frequency range [44], [52] employed impulse tests on a hemispherical electrode with an auxiliary current return mesh electrode using 3 and 4-terminals setups. Impulses of different front and tail times were applied, and soil impedance $Z(\omega)$ was obtained applying FFT to the measured voltage and current signals. The bulk soil parameters were calculated assuming hemispherical current propagation. Kuklin has developed an intricate device capable of measurement of soil parameters in-situ using an array of voltage and current electrodes [45]. Clark et al. [53] used a number of different test instruments to conduct variable frequency tests on rods and grids submerged in a lake and found significant current density dependence of electrode impedance at low current magnitudes. Field tests on ground rods were carried out by Gayeb et al. [54], confirming the significant effect of electrode material type and current density on the measured impedance using a 3-terminal test arrangement.

C. Comparative analysis of frequency dependence

1) Resistivity

Fig. 2a presents selected results from investigators of measured apparent resistivity of soils and electrolytic solutions digitized using OriginPro® software. Against each curve representing a set of results for the soil samples, the percentage soil moisture is indicated. For cases where the test medium is composed entirely of electrolyte, each curve is indicated by its molar ionic concentration. It can be seen from the figure that, generally, as soil moisture increases from 0% to 20-30%, the resistivity falls with frequency by orders of magnitude. While this is a valid general trend, it can also be seen that different soil samples having the same moisture content may exhibit significantly different resistivities; e.g. the resistivity at 100Hz measured by Ward and Jiracek [7] with 4% moisture is at least an order of magnitude greater than that of a sample of the same moisture content from Scott et al. [5]. Similarly, samples having very different moisture contents are shown to have similar resistivity; e.g. the results of Mallon for 9% moisture compared with those of Smith-Rose at 39% [2], [15]. The microstructure of the material, the amount of water it contains, the ionic concentration of salts in the water or the resistivity of water in the material and the amount of clay in the material are some of the factors which control the conduction through the soil [12]. Fig. 3 shows the trend of reducing resistivity with moisture (taking values at 100Hz), and there is considerable variation among individual results.

Dry soil samples such as sandy soil tested by He et al. [43], volcanic ash by Ward and Jiracek et al. [7] and natural silica sands by Datsios et al. [37] are characterized by an almost inverse reduction in resistivity with frequency, falling at a rate of approximately one decade per decade. For samples having between 0.3% and 3-4% moisture, the results indicate a lower rate of fall of resistivity with frequency, e.g. [15]. When soil moisture exceeds 3-4%, a distinct plateau region between about 100Hz to 1 MHz in resistivity is found by most investigators. An increasing trend in resistivity with frequency for high moisture content soils, built into the universal model developed by Longmire and Smith [13] and, based on Scott's results [10], it is not borne out by the other results shown in Fig. 2a. Either side of the plateau region, for soils with moisture, two distinct non-linear regions are evident. First, on the low frequency side of the plateau, there is an increase in resistivity as frequency falls, and this may be attributed to the EEI. This is clearly illustrated by results from a soil sample tested by Garrouch and Sharma [4] using a 2-terminal and a 4-terminal test systems on the same sample. The upper (dotted red) curve shown in Fig. 2a, corresponding to the 2-terminal tests, exhibits a clear upturn starting at about 1kHz as frequency decreases, while the lower curve from the 4-terminal test remains flat.

The EEI effect can be seen from a different perspective with results of Scott et al. [5], where a pair of 4%-moisture curves (solid blue) for the same soil sample are shown in Fig. 2a and where the upper curve corresponds to a test with sliver electrodes, while the lower curve is for non-polarizing electrodes. While the latter curve is flat down to 100Hz, the upper curve has a rising resistivity as frequency decreases from about a few tens of kilohertz downwards, indicating an EEI effect. The low frequency upturn trends are considerably more marked with single ionic solutions compared with soils, as can be seem from the results of Duarte et al. [34]; in these tests, the electrodes were made of titanium. The field tests by Alipio and Visacro [55] show that, while exhibiting the same low frequency resistance, different soils may have different high frequency downturn trends (dot-dash blue curves).

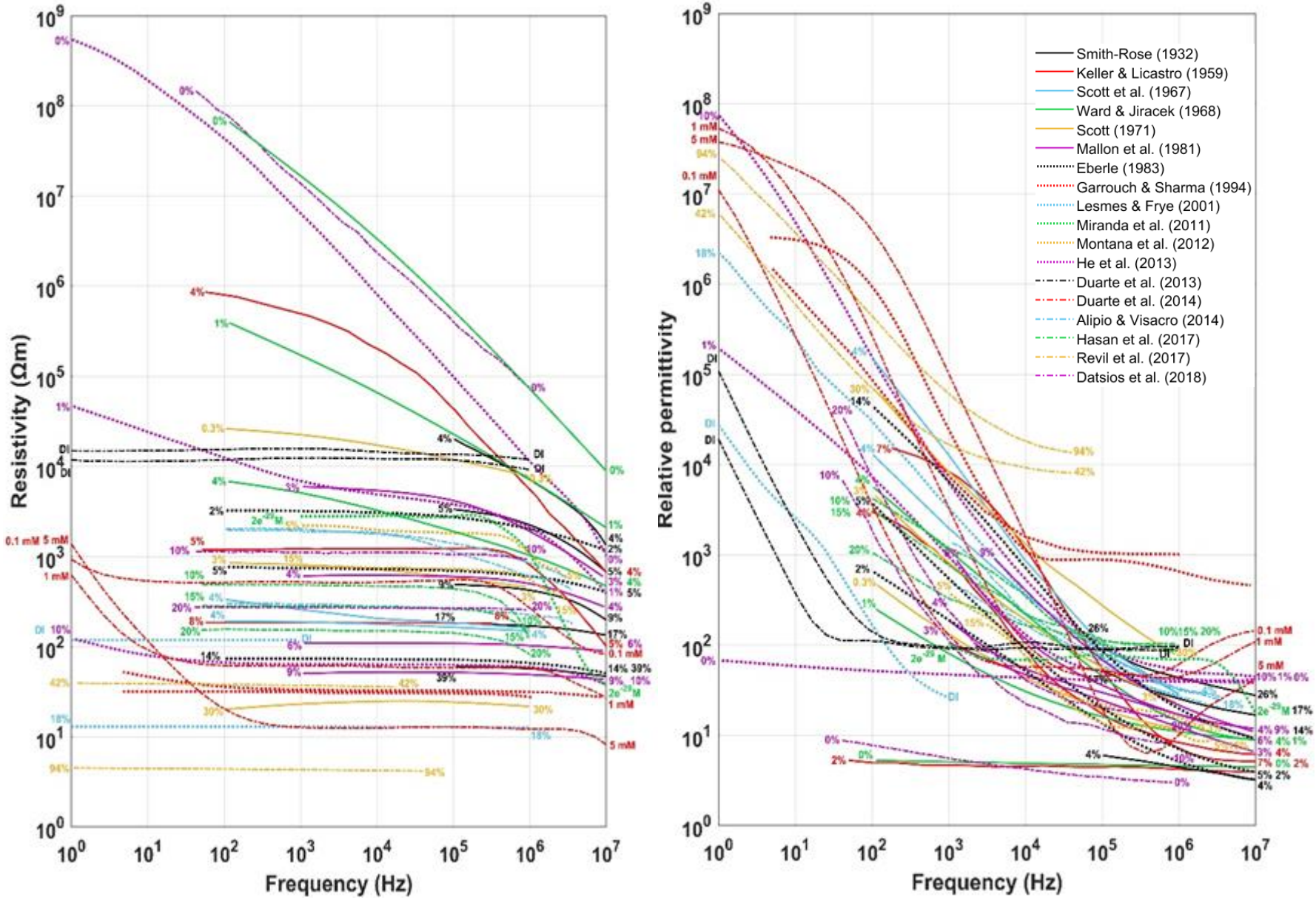

(a) (b)

Fig. 2. Selected apparent soil parameter frequency response test results: (a) resistivity, (b) relative permittivity

A second non-linear region in resistivity appears above approximately 100kHz, and it can be seen that the precise downturn frequency (-3dB) from the plateau region varies from study to study. Results from Smith-Rose [2] indicate that the downturn frequency increases with moisture content, and this trend is also confirmed by Eberle [16], Hasan et al. [35] and by Visacro and Alipio [44] from field tests. It is noted that an apparent high frequency downturn characteristic is sometimes an artifact of the test system rather than representative of the intrinsic behavior of the test medium. This can be illustrated, for example, from the pair of curves from Garrouch and Sharma [4] where each of this pair exhibit dissimilar high frequency roll-offs which can be attributed to the different measurement systems employed to test the same sample.

Generalized models have been proposed to describe the resistivity dispersion of soils [12] but they have acknowledged that shapes of curves from different samples are dissimilar due to factors including the EEI effect and clay content which makes accurate generalization difficult. Based on the current set of results, equivalent circuit models accounting for EEI and the bulk medium elements are being analyzed in detail for both electrolyte and soil mediums and the results will be reported in future. Returning to Fig. 3, clay soils tend to have lower resistivity at low frequency, probably due the formation of an exchange cationic cloud around the clay particles which adds to the free electrolyte ionic movement [12], [17].

2) Permittivity

A corresponding set of relative permittivity dispersion data is shown in Fig. 2b. From the figure, a general trend of increasing relative permittivity is observed with soil moisture content/ ionic concentration. Fig. 3 shows the trend of increase in relative permittivity with moisture at 100Hz; there is a significant spread around the trend line and particularly so at lower moisture values (<10%). Nevertheless, results for clay samples indicate generally much higher values of permittivity which may be explained by clay counterions displacement and electrolyte blockage by clay site membranes.

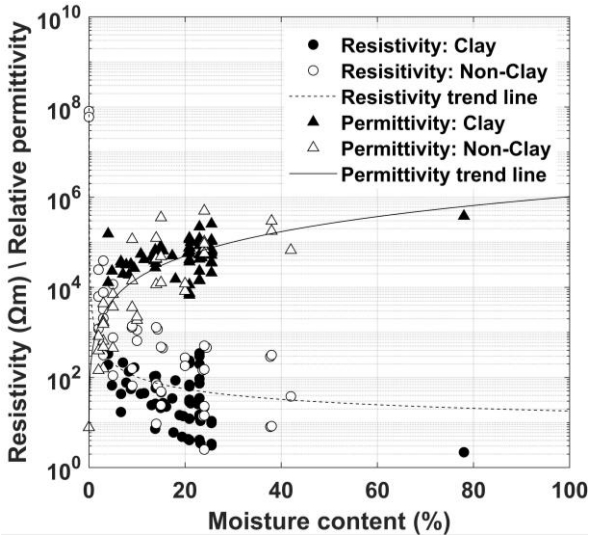

Fig. 3. Resistivity and permittivity of clay and non-clay soils at 100Hz against % moisture

As shown in Fig. 2b, for dry samples or some samples with a very low moisture content [3], [7], [37], [43], relative permittivity is low and the curves are quite flat over their tested range of frequencies. The results for deionized water [33] indicate a long plateau region at a value of about 100 from high frequency down to about 100 Hz below which there is a sharp upturn in relative permittivity attributable to the EEI effect. However, elevated values of permittivity below the upturn frequency may also be due to small phase angles at such low frequencies, which may affect accuracy, as reported in [39].

The sharp fall in apparent relative permittivity with frequency is also evident as a general trend for most moist soils [28], [36], [43]. However, the initial rate of reduction (roll off) is not consistent among the different tests, ranging from about ~50 to ~95 percent/decade. This reduction is linear until at higher frequencies where the rate of reduction decreases and the relative permittivity for some soils tends to an asymptotic value at 1kHz [4], [36], 10kHz [35], 1MHz [43] and beyond 10MHz for others. The relaxation theory model was used [12] in an attempt to predict permittivity values from resistivity measurements. However, this model is based on a classical dielectric with losses and does not account for EEI polarization, clay particle charging effects and the general Maxwell-Wagner effect due to inhomogeneities.

D. Current density dependence of soil/ electrolyte parameters

Ragheb and Geddes [19] carried out laboratory tests on electrolytes energized through a variety of metal electrode materials including copper, aluminum, stainless steel and platinum. The effect of current density on the electrode/electrolyte interface resistance and capacitance was investigated, where the EEI contributed most to the total impedance. The results showed marked reductions in measured resistance with current density over the range 1 to 200 A/m^2 with the effect most pronounced at low frequencies (100Hz). Beyond a few thousand Hz, the current density effect is not seen. Platinum electrodes exhibited a plateau region of resistance until a threshold frequency where the resistance suddenly dropped. Aluminium electrodes, however, exhibited an increase in resistance with current density at low frequencies before reaching a peak and followed by a fall-off. Such contrasting behavior was also seen between the measured resistance of copper and aluminium electrodes with current density in large scale field tests on electrodes submersed in a lake [53]. Field tests on a range of electrodes (copper rod, copper grid and a full size 275 kV steel transmission tower base) also revealed marked reductions in measured impedance with current density [56]. More recently, field tests were carried out [54] comparing three-terminal and four-terminal configurations to investigate the EEI effect using different electrode materials under switched DC and variable frequency AC. The 3-terminal tests revealed dependence of impedance on current density in the range 0.1 to 5 A/m^2 while no such variation was seen for the four terminal tests, confirming that the measured non-linearity was due to the EEI effect. Aluminium electrodes were found to have by far the greatest

dependence on current density followed by copper and stainless steel. Hasan et al. [35] carried out laboratory tests investigating the effect of current magnitude and frequency measured impedance of soil samples using a two-terminal arrangement with copper electrodes. The results indicate significant measured impedance variation with current magnitude under both sinusoidal and impulse energizations.

IV. EXPERIMENTAL INVESTIGATION

A. Test cell and electrode materials

2-terminal impedance spectroscopy was carried out using a purposely-built acrylic cuboidal test cell as shown in Fig. 4. The 2-terminal arrangement enables capturing the EEI effects to compare with previous tests reported in the reviewed literature, the majority of which adopted this setup. Subsequent tests will employ the 4-terminal setup, and as noted [27], this introduces complexities in terms of obtaining accurate measurement, particularly in terms of the type and configuration of the potential electrodes. Interchangeable electrodes (20 cm x 20 cm x 3 cm) are placed on opposite faces of the test cell to investigate the effect of different electrode materials. Such dimensions were chosen to maintain a reasonably uniform electric field and current density throughout the test cell and to achieve relatively high values of current density. In particular, the longer current path length offers the advantage to allow sufficient space to position additional potential electrodes for 4-terminal tests that will be reported in a subsequent paper. Another advantage of this design is to allow a straightforward interchange of current electrodes. A substantially uniform distribution of electric field and current density throughout the test cell with deionized water as medium was verified by COMSOL simulations. It is known that with a medium of permittivity greater than that of air in the cell, the electric field lines tend to be confined within the medium [57], [58], thereby reducing fringing. In the analysis we use to derive the resistivity and permittivity of the medium, a uniform field distribution is assumed and fringing effects are neglected. It is to be noted that the error that may be introduced due to such an assumption has not been accounted for in the present work. The different electrode materials are listed in Table II. Copper is used as the preferred material in dedicated grounding installations and steel is often used a fortuitous ground electrode in reinforced concrete of buildings and in transmission line tower footings and where such metalwork is bonded to the power system earth. Aluminum and platinum were chosen for comparative testing since they are known to exhibit large and small EEI effects respectively [5], [59].

Two distinct test media were used. First, electrolytic solutions of different concentrations prepared from anhydrous sodium sulfate (Na_2SO_4) and deionized water. An ionic solution was chosen because it ensures consistent and intimate contact between the conducting medium and the metallic plates. This is useful when comparing the effects of different metal electrodes. Furthermore, use of a single salt solution reduces the complexity of the EEI effect. This particular solution was chosen because sodium has a low reduction potential compared with the test electrode metals, and the electrochemical reactions between the electrodes and electrolyte are minimized accordingly. In addition to deionized water, four solutions were prepared with salt concentrations ranging from $1{\cdot}10^{-5}$ M to $1{\cdot}10^{-3}$ M which provided a test medium with mid-frequency nominal resistivities ranging from about 50 Ωm to 10kΩm. Nominal resistivity reduces approximately by one decade for each decade increase in molar concentration. Secondly, a natural sand (as per local condition) was used comprising 67% carbonates (various types of grains) and 33% siliciclastic materials (quartz, feldspars, and rock fragments). The sample has a unimodal grain size distribution with a minor positive skew and a mean particle size of 250μm.

TABLE II -ELECTRODE MATERIALS

Electrode type	Symbol	Material specification
Copper	Cu	C11000 - 99.93%
Stainless steel	SS	SS - 304
Aluminium	Al	6061 - 96.78%
Platinized titanium	Pt	B265 - 99.4%; 5μm coating

TABLE III -TEST SYSTEM SOURCE PARAMETERS

Test system	VOLTAGE MAGNITUDE (V)	Frequency range (Hz)	Current density limit (A/m^2)
Gamry Interface 1000E™	10^{-5} – 2.3	10^{-6} – 10^{6}	2.5
IMS	0.5-100	$0.5\text{-}2{\cdot}10^{6}$	15
Bode 100	0.007-1	$1\text{-}40{\cdot}10^{6}$	0.5

Sand samples were prepared by first placing the test sample in an oven (T = 110°C) for 72 hours and weighed to provide the dry sample weight. Weighed quantities of deionized water (ρ ~ 11 kΩm) were mixed to provide samples in terms of % water content by weight (saturation/moisture). Five samples were prepared with moistures ranging from 0.2 % to 2.6% to match approximately the nominal resistivities of the prepared electrolytic solutions and deionized water. In addition, dry sand was also tested which gave a much higher resistivity. Sample temperature was periodically monitored and it was found to be 21ºC ± 2ºC. The soil packing and distribution of moisture in soil affects the measured values. To ensure minimum effect of these factors soil was meticulously hand mixed to ensure uniform distribution of moisture and packing was done using a roller.

B. Test sources and instrumentation

Three systems were used to achieve the range of frequency and current density (Table III): (i) Gamry Interface 1000TM potentiostat, a proprietary electrochemical test system, (ii) a Bode 100 test instrument and (iii) an in-house assembled

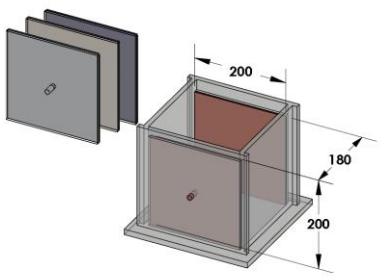

Fig. 4. Test cell for 2-terminal measurements of soil samples and aqueous salt solutions (dimensions in mm)

impedance measurement system (IMS) comprising a precision oscillator, a wideband power amplifier and an oscilloscope (Fig. 5). The three test instruments show close agreement in their common ranges of voltage, frequency and current density.

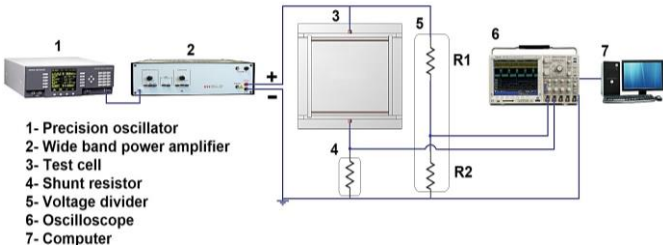

Fig. 5. IMS experimental test setup

Precision resistors were used to measure the voltage across and current flow through the test cell, as shown and shielded to minimize stray capacitances and lead inductances [60]. The Gamry, Bode100 and the IMS test measurement systems were set to perform automatic frequency sweeps at specified voltages. The IMS was controlled using a LabView interface with time domain voltage and current signals captured by an oscilloscope, then processed in MATLAB® using a phase-sensitive detection technique for noise reduction and conversion to phasor quantities. Accordingly, the quotient of the phasor voltage and current yields the complex impedance of the test cell. The three instruments gave approximately similar results within their common frequency range, as shown in Fig. 6, both in terms of impedance magnitude and phase angle. Nevertheless, the Gamry instrument was used from 1Hz to 100 kHz because of its superior noise rejection capability, while the Bode 100 was utilized for its higher frequency range and at frequencies where interference was less problematic (100 kHz to 10 MHz). The IMS system was used for the higher current tests and for phase angle verification at low current and low frequencies. Such phase angle verification, based on the average power method and phase sensitive detection, were carried out due to the high sensitivity of relative permittivity values to small errors in phase angle measurement of conducting media where the capacitive current is significantly smaller than the conduction component.

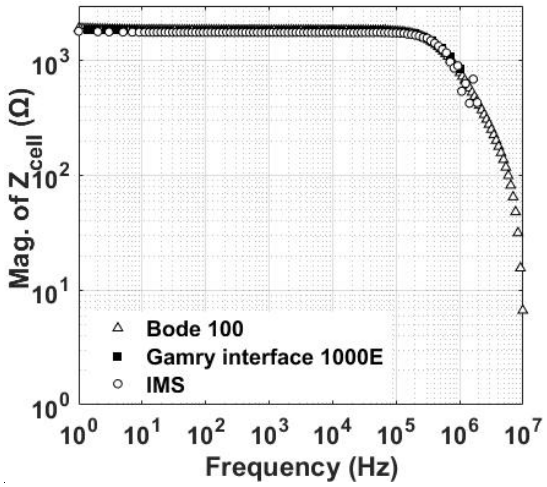

Fig. 6. Impedance spectroscopy data for 0.1mM electrolyte with SS electrodes and different test systems (a) Magnitude and (b) phase angle.

C. Test results - calculated apparent resistivity and relative permittivity

Fig. 7 shows the calculated apparent soil resistivity (ρ_{eff}) (Fig.7a) and permittivity ($\varepsilon_{r(eff)}$) (Fig.7b) for platinized electrodes obtained from the swept frequency test data using the Gamry and Bode instruments at 1 V. These parameters were calculated from the measured complex admittance of the test cell (Y_{cell}) using the following equations, and adopting a parallel R-C equivalent circuit for the cell:

$$\rho_{eff}(\omega) = (Re(Y_{cell}))^{-1} \cdot (A/d) \quad (4)$$

$$\varepsilon_{r(eff)}(\omega) = Im(Y_{cell}) \cdot (d/A)(1/\omega\varepsilon_0) \quad (5)$$

where d is the distance between the electrodes, A the cross-sectional area of the electrodes, f the test frequency and ε_0 the permittivity of free space.

1) Solutions of different ionic concentration

Considering first the resistivity of the aqueous solutions (blue lines) in Fig. 7a, the plots for all solutions have an extended plateau region of resistivity down to 1 Hz. This contrasts with Duarte's results (Fig. 2a) which show a significant upturn in apparent resistivity at low frequencies. The difference could be due to the different electrode materials: platinum in this work and titanium in [34]. For deionized water, a flat response is seen down to the lowest test frequency, which is in agreement with previous results [33]. Above 1MHz, there is a downturn in apparent resistivity for all solution concentrations, and the downturn frequency increases with the ionic concentration.

Regarding permittivity (Fig. 7b), the results presented here with platinized electrodes (Fig. 7b) show that the relative permittivity for all solution concentrations converge to a value of ~80 (permittivity of deionized water, shown as dashed line) above 1kHz, in contrast to the results, for example, of [34] where oscillations are seen at high frequency. The small upturn above 2MHz seen in Fig. 7b is thought to be caused by circuit inductance. Below 1kHz, there is an upturn in permittivity as frequency falls. The frequency at which such upturn occurs is higher for solutions of higher concentration.

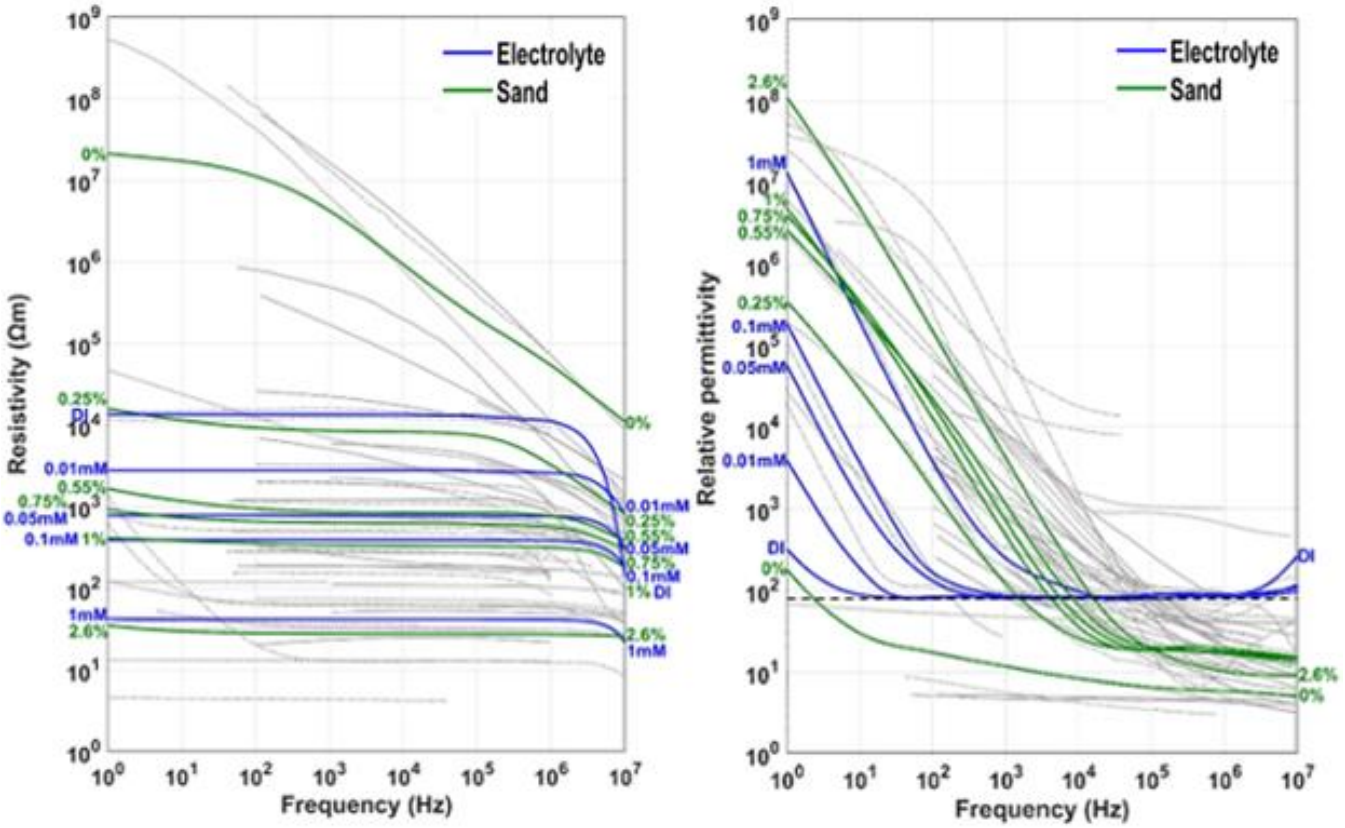

(a) (b)

Fig. 7. Soil and electrolyte parameter dispersion with platinized electrodes: (a) resistivity, (b) rel. permittivity (background in grey: previously published results in grey), dotted line: Theoretical permittivity of de-ionized water.

2) Sand samples of different moisture content

The corresponding set of results for sand samples of different moisture contents are shown in Fig 7a and 7b. Similar trends to those of the ionic solutions appear in resistivity and permittivity. Some key differences, however, are apparent: (i) there is an upturn in apparent resistivity in the lower frequency region of the soil samples compared with the electrolyte solutions and the upturn starts at a higher frequency for lower moisture contents, (ii) the value of relative permittivity for soils tends to an asymptotic value which is lower than 80 and whose value is different for different moisture levels. The high frequency asymptote below 80 is not seen in the results of [4], [10], [34], [35]. For dry sand, the high frequency relative permittivity, ε_r, is below 10. In the mid-range of frequency, the values of relative permittivity for sand are higher than those for the sodium sulphate solutions of comparable mid-range resistivity value, seen as a shift to the right in the graphs. Such elevated values may not, however, reflect the intrinsic values of the medium but a greater relative contribution of the electrode-electrolyte interface effect. In the case of soils, there may be a less intimate contact between the bulk medium and the electrodes compared with the electrolytic solutions, thereby increasing the EEI effect. It should also be noted that the values of calculated relative permittivity for conducting soils are highly sensitive to small inaccuracies in phase angle measurement.

3) Effect of electrode material

Fig. 8 shows the effect of electrode material on effective soil/ solution parameters measured at 1V. For electrolytic solutions, Fig. 8a shows that there is relatively small effect of electrode material on apparent resistivity. The aluminium electrodes produce a small upturn in resistivity below 10Hz in contrast with the other electrodes. However, Fig. 8b shows a marked difference in relative permittivity of electrolytes with the different electrodes in the low frequency range. The 'low-frequency upturn' shifts to the left as a function of the position of the metal in the electrochemical series, with platinum as the noble metal least susceptible to electrochemical reaction. The results in Fig. 8c for the sand samples indicate a greater impact of electrode material on resistivity at low frequency. In contrast to the test results on the electrolytes, there was less variation in relative permittivity with electrode material and, unexpectedly, copper electrodes gave lower values of permittivity. It may be borne in mind that the process of interchanging the electrodes for the soil tests means that an exact like-for-like comparison in the testing of different electrode materials is difficult because of differences in compaction and contact between the test medium and electrodes.

4) Effect of current density

Using the in-house developed IMS test system that can generate higher test voltages than the proprietary test equipment, the effect of current density was investigated for stainless steel test electrodes with sand media having 0.25 wt.% moisture content. The results are shown in Fig. 9 for current

density in the range 1-35 mA/m^2. The displayed frequency range is curtailed above 3 kHz since the current density effect is negligible above this value. The results are extended here below 1Hz to illustrate the increasing divergence of results attributable to the interfacial effect. With reference to Fig. 9a, below 10 kHz the resistivity increases with reducing frequency because of a progressing assimilation of more of the contribution of EEI impedance; most significantly, the charge transfer resistance and the electrochemical double-layer. Therefore, bulk resistivity could be overestimated from tests using low current density. Similarly, the effect of current density is also significant on measured relative permittivity. As seen in Fig. 9b, increasing the current density from 1 to 35 mA/m^2 reduces the apparent permittivity by almost one decade. Following an error calculation considering instrument tolerances, the estimated maximum error in the measurements is 5%. The variations shown in Fig. 8 and Fig. 9 are beyond the measurements uncertainty and are solely attributable to EEI effect.

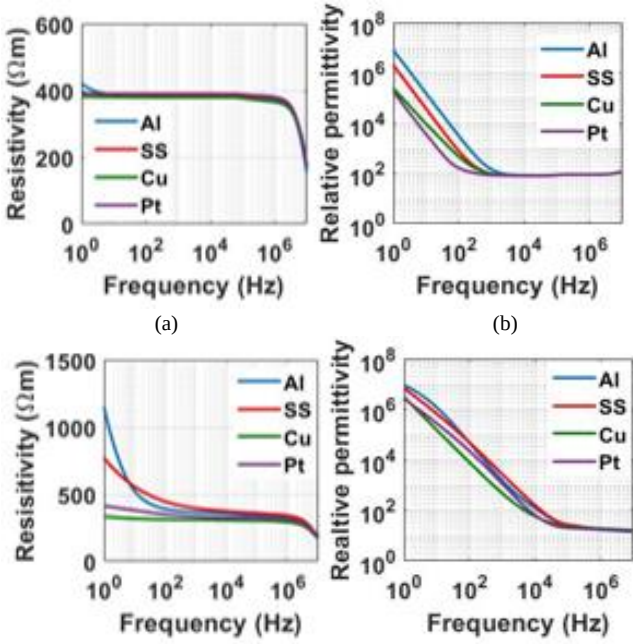

Fig. 8. Effect of electrode material on measured apparent parameters: (a) resistivity- electrolytic solution (0.1mM), (b) permittivity - electrolytic solution (0.1mM), (c) resistivity- sand (1w.%) (d) Permittivity – sand

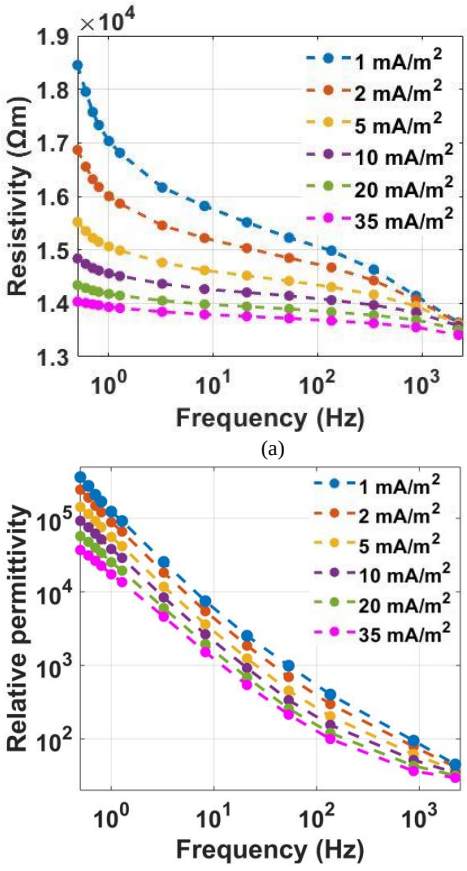

Fig. 9. Measured apparent parameters with stainless steel electrodes at different current densities: (a) resistivity (b) permittivity (0.25 wt.% sand)

The combined effect of frequency and current density on soil parameters is shown in Fig. 10 as a surface plot and the results highlight that the EEI effect is most prominent at low current density and low frequency. Above ~40mA/m^2 and ~10 kHz, the resistivity and permittivity are not significantly affected by current density for this specific case shown.

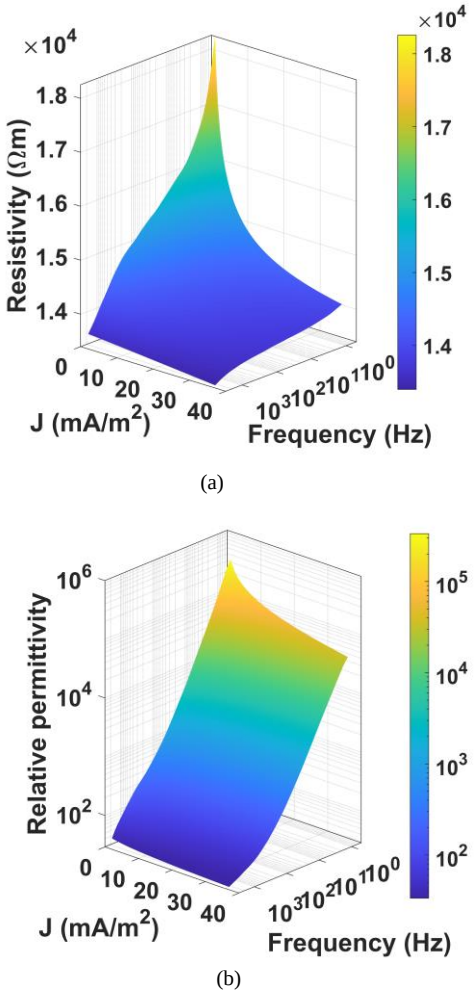

Fig. 10. Measured resistivity and permittivity with stainless steel electrodes as a function of frequency and current density (0.25 wt.% sand)

5) Comparison of measured parameters with proposed CIGRE equations

The values of soil parameters obtained from experiment in this work at different moisture content are compared with two sets of published equations from CIGRE TB781, as shown in Fig. 11. CIGRE equations 5.1 and 5.2 of that document were obtained by curve fitting to an extensive set of data obtained from field tests [44] while later revised equations, 5.3 and 5.4, are described as accounting for the Kramers-Kronig relation. With reference to Equations 5.1 to 5.4 from CIGRE TB781 the curves for resistivity and relative permittivity shown in Fig. 11 were obtained from these equations using ρ_o measured at 100 Hz.

With reference to Fig.11a, the results from the current work suggests a wider plateau region for resistivity and a downturn in resistivity at a higher frequency. With regard to the relative permittivity, as shown in Fig. 11b, the current work indicates a more definite asymptotic value above 100 kHz.

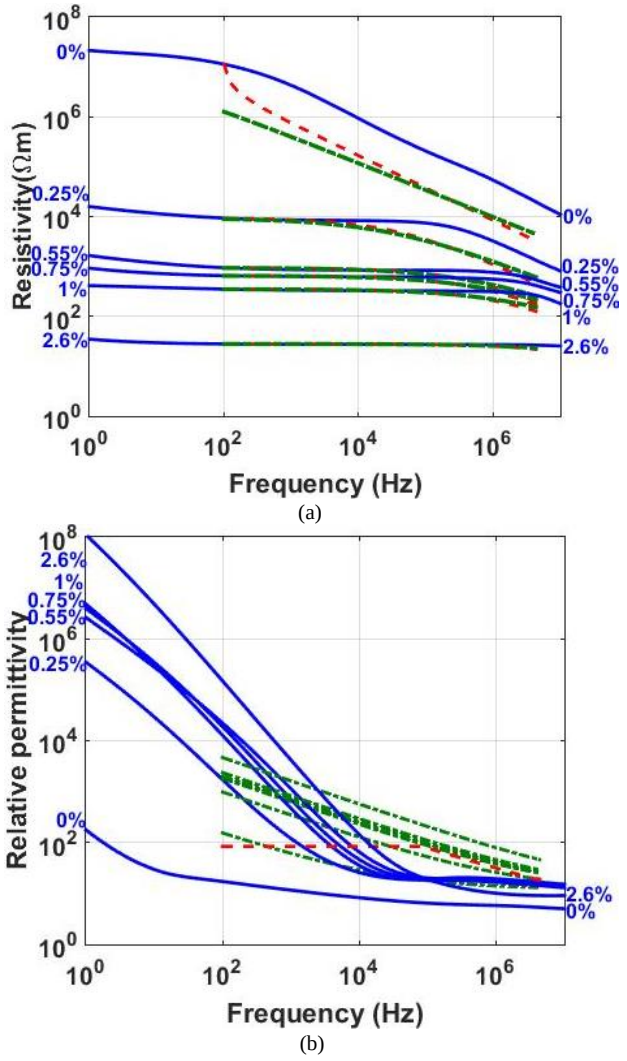

Fig. 11. Frequency response of soil parameters with platinized electrodes compared with Equations in CIGRE TB781: (a) resistivity, (b) permittivity.

V. Conclusions

A review of previous work investigating the variation of resistivity and permittivity in soil and electrolytes with frequency (up to 10MHz) has revealed wide differences in measured values which may be partly attributed to the different test setups, electrode materials and energization. The impact of the EEI effects on permittivity results is highlighted.

The present work has employed platinized electrodes to minimize the EEI effect and used a test set up with larger surface area electrodes. Furthermore, a higher test voltage was used to facilitate the investigation of the effect of current density. The findings of the present work indicate:

- the resistivity of aqueous solutions exhibits a large plateau region down to 1 Hz in contrast to previous results which indicated a significant upturn in apparent resistivity at low frequencies.
- at high frequency, above 1MHz, there is a downturn in apparent resistivity for all solution concentrations and the downturn frequency is related to ionic concentration where a higher concentration yields a higher downturn frequency.
- the permittivity of aqueous solutions using platinized electrodes indicate a rapid fall with frequency and converging to a value of 80 above 1kHz for all solution concentrations. The low frequency upturn in permittivity is proportional to solution concentration with higher concentrations giving upturns at higher frequencies.
- regarding the frequency response of soil resistivity, the broad trend was found similar to that of the aqueous solutions with the presence of a long plateau region but, with soil, there is a significant upturn in apparent resistivity in the low frequency region which may be due to the electrode-electrolyte interface even with the platinized electrodes; the upturn starts at a higher frequency for lower moisture contents.
- the value of relative permittivity of sand samples tends to an asymptotic value which is lower than 80.
- in the mid-range frequencies, the levels of relative permittivity for sand are higher than those seen for the sodium sulphate solutions of comparable mid-range resistivity value (a shift to the right in the graphs). Such elevated values may not, however, reflect the intrinsic value of the medium but the electrode-electrolyte interface effect.
- the results of current density variation revealed that resistivity may be overestimated when testing at low current density.
- the effect of current density on measured relative permittivity was also found to be significant and, as current density is increased from 1 to 35 mA/m^2, the apparent permittivity reduces by almost one decade.
- a comparison of the measured frequency responses soil parameters with CIGRE models indicate significant differences in both resistivity and permittivity.
- further work is being carried focusing on the isolation of the electrode-soil interface impedance using 4-terminal tests on the same and new test samples including those composed of clay material. Also, the influence of test circuit inductance on measured parameter values at high frequencies is investigated and compensation measures quantified.

APPENDIX I

The following equations describe the bulk parameters of any medium which determine the response of such medium to the applied electric field. The total current density at a point, J_t, in a medium is described by

$$J_t = J_c + J_d \tag{I.1}$$

where

$$J_c = \sigma^* E \tag{I.2}$$

and

$$J_d = \frac{\partial D}{\partial t} \tag{I.3}$$

where J_c is the conduction current density, σ^* is the complex conductivity and J_d is the displacement current density. Substituting (I.2) and (I.3) into (I.1) gives

$$J_t = \sigma^* E + \frac{\partial D}{\partial t} \tag{I.4}$$

where σ^* has real and imaginary components σ' and σ'' given by

$$\sigma^* = \sigma' + j\sigma'' \tag{I.5}$$

and

$$D = \epsilon^* E \tag{I.6}$$

where σ^* is the complex permittivity of the medium. Substituting for D into (I.4) gives

$$J_t = \sigma^* E + \epsilon^* \frac{\partial E}{\partial t} \tag{I.7}$$

where, conventionally,

$$\epsilon^* = \epsilon' - j\epsilon'' \tag{I.8}$$

Assuming sinusoidal energization,

$$\tilde{E} = E_0 e^{j\omega t} \tag{I.9}$$

Equation (I.7) becomes,

$$\widetilde{J_t} = [\sigma^* + j\omega\epsilon^*]\tilde{E} \tag{I.10}$$

Substituting (I.5) and (I.8) into (I.10) gives,

$$\widetilde{J_t} = [\sigma' + j\sigma'' + j\omega(\epsilon' - j\epsilon'')]\tilde{E} \tag{I.11}$$

$$\widetilde{J_t} = [\sigma' + \omega\epsilon'' + j(\sigma'' + \omega\epsilon')]\tilde{E} \tag{I.12}$$

$$\widetilde{J_t} = \left[\sigma' + \epsilon'' + j\omega\left(\frac{\sigma''}{\omega} + \epsilon'\right)\right]\tilde{E} \tag{I.13}$$

From (I.13), an effective conductivity, σ_{eff} and permittivity, ε_{eff} can be defined where

$$\widetilde{J_t} = \left[\sigma_{eff} + j\omega\epsilon_{eff}\right)\tilde{E} \tag{I.14}$$

and

$$\sigma_{eff} = \sigma' + \omega\epsilon'' \tag{I.15}$$

and

$$\epsilon_{eff} = \frac{\sigma''}{\omega} + \epsilon' \tag{I.16}$$

and with

$$\epsilon'' = \epsilon_r''\epsilon_0 \quad \text{and} \quad \epsilon' = \epsilon_r'\epsilon_0 \tag{I.17), (I.18}$$

(I.15) and (I.16) may be written as

$$\sigma_{eff} = \sigma' + \omega\epsilon_r''\epsilon_0 \tag{I.19}$$

and

$$\epsilon_{eff} = \frac{\sigma''}{\omega} + \epsilon_r'\epsilon_0 \tag{I.20}$$

Additionally, (I.14) can be written in terms of an effective relative permittivity, where

$$\widetilde{J_t} = \left[\sigma_{eff} + j\omega\epsilon_{r(eff)}\epsilon_0\right)\tilde{E} \tag{I.21}$$

and where

$$\epsilon_{r(eff)} = \frac{\sigma''}{\omega\epsilon_0} + \epsilon_r' \tag{I.22}$$

The effective values, σ_{eff}, ε_{eff}, and $\varepsilon_{r(eff)}$ lend themselves to be calculated from experimentally determined soil impedance obtained from the in-phase and quadrature components of the quotient of phasor current and voltage.

The conduction and displacement components of (I.14) are sometimes combined and expressed as a single effective complex conductance [32] where

$$\widetilde{J_t} = \sigma_{eff}^* \tilde{E} \tag{I.23}$$

where

$$\epsilon_{eff}^* = \sigma_{eff} + j\omega\epsilon_{eff} \tag{I.24}$$

and an effective quadrature component of complex conductance may be defined where,

$$\sigma_{eff}'' = \omega\epsilon_{eff} = \sigma'' + \omega\epsilon' \tag{I.25}$$

De Lima and Sharma [27] adopt a negative sign convention for the quadrature component in (I.10) giving $\widetilde{J_t} = [\sigma^* - j\omega\varepsilon^*]\tilde{E}$ and Revil [32] expresses (I.24) as $\sigma_{eff}^* = \sigma_{eff} - j\omega\varepsilon_{eff}$.

ACKNOWLEDGMENT

The research was supported by the APEC center at Khalifa University. The authors thank Dr A. Ceriani from the Dept. of Earth Sciences at Khalifa University for the physical analysis of the sand samples.

REFERENCES

[1] J. H. Scott, "Electrical and Magnetic Properties of Rock and Soil," U. S. Dep. Inter. Geol. Surv., Denver, USA, Open-File Rep. 83-915, 1983.

[2] R. L. Smith-Rose, "The Electrical Properties of Soil for Alternating Currents at Radio Frequencies," *Proc. R. Soc. London*, vol. A-140, pp. 359–377, 1932.

[3] G. V. Keller and P. H. Licastro, "Dielectric Constant and Electrical Resistivity of Natural-State Cores," U. S. Dep. Inter. Geol. Surv., Denver, USA, Geol. Surv. Bull. 1052-H, 1959.

[4] A. A. Garrouch and M. M. Sharma, "The influence of clay content, salinity, stress, and wettability on the dielectric properties of brine-saturated rocks: 10 Hz to 10 MHz," *Geophysics*, vol. 59, no. 6, pp. 909–917, 1994.

[5] J. H. Scott, R. D. Carroll, and D. R. Cunningham, "Dielectric constant and electrical conductivity measurements of moist rock: a new laboratory method," *J. Geophys. Res.*, vol. 72, no. 20, pp. 5101–5115, 1967.

[6] M. M. Judy, "Separation of electrode and polarization medium impedances in two-terminal measurements," U. S. Dep. Inter. Geol. Surv., Denver, USA, Technical letter special project -21, 1967.

[7] S. H. Ward, G. R. Jiracek, and W. I. Linlor, "Electromagnetic reflection from a plane-layered lunar model," *J. Geophys. Res.*, vol. 73, no. 4, pp. 1355–1372, 1968.

[8] W. R. Judy and M. M. Eberle, "A laboratory method for the measurement of the dielectric constant of rock and soil samples in the freqeuncy range 10^2 - 10^8 Hertz," U. S. Dep. Inter. Geol. Surv., Denver, USA, Sensor and Simulation Notes Note 88, 1969.

[9] B. D. Fuller and S. H. Ward, "Linear System Description of the Electrical Parameters of Rocks," *IEEE Trans. Geosci. Electron.*, vol. 8, no. 1, pp. 7–18, 1970.

[10] J. H. Scott, "Electrical and Magnetic properties of Rock and Soils," AFWL, Electromagnetic pulse theoretical notes (2-1) note -18, 1971.

[11] R. N. Grubb and J. R. Wait, "In-situ measurements of the complex propogation constant in rocks for frequencies from 1 to 10 MHz," 1971.

[12] R. C. Bigelow and W. R. Eberle, "Empirical predicted curves for resistivity and conductivity of earth materials: 100 Hz to 100 MHz," U. S. Dep. Inter. Geol. Surv., Denver, USA, Special project - 30, 1972.

[13] C. L. Longmire and K. S. Smith, "A universal impedance for soils,"

Def. Nucl. Agency, Washington DC, USA, Rep. DNA 3788T, 1975.
[14] J. P. Poley, J. J. Nooteboom, and P. J. de Waal, "Use of V. H. F. Dielectric Measurements for Borehole Formation Analysis," *Log Anal.*, vol. 19, no. 3, pp. 8–30, 1978.
[15] C. Mallon, "Low field electrical characteristics of soil," JAYCOR, San Deigo, USA, Theor. Notes 315, 1981.
[16] W. R. Eberle, "The effects of water content and water resistivity on dispersion of resistivity and dielectric constant in quartz sand in the frequency range 10^2 - 10^8 Hz," U. S. Dep. Inter. Geol. Surv., Denver, USA, Open-File Rep. 83-914, 1983.
[17] H. J. Waxman and M. H. Vinegar, "Induced polarization of shaly sands," *Geophysics*, vol. 49, no. 8, pp. 1267–1287, 1984.
[18] R. J. Knight and A. Nur, "Dielectric constants of sandstones, 60 kHz to 4 MHz," *Geophysics*, vol. 52, no. 5, pp. 644–654, 1987.
[19] T. Ragheb and L. A. Geddes, "Electrical properties of metallic electrodes," *Med. Biol. Eng. Comput.*, vol. 28, pp. 182–186, 1990.
[20] T. Ragheb and L. A. Geddes, "The polarization impedance of common electrode metals operated at low current density," *Ann. Biomed. Eng.*, vol. 19, pp. 151–163, 1991.
[21] CIGRE WG C4.407, "Lightning parameters for engineering applications," Technical Brouchre- 549, 2013.
[22] M. A. Laughton and D. J. Warne, *Electrical Engineer's Reference Book*, 16th ed. Elsevier, 2003.
[23] M. Nazari, R. Moini, S. Fortin, F. P. Dawalibi, and F. Rachidi, "Impact of Frequency-Dependent Soil Models on Grounding System Performance for Direct and Indirect Lightning Strikes," *IEEE Trans. Electromagn. Compat.*, vol. 63, no. 1, pp. 134–144, Feb. 2021.
[24] H. Griffiths and N. Pilling, "Earthing," in *Advances in High Voltage Engineering*, 1st ed., A. Haddad and D. Warne, Eds. London: The IET, 2004, pp. 349–402.
[25] "IEEE Guide for safety in AC substation grounding," IEEE Std 80, 2013.
[26] "IEEE Guide for Measuring Earth Resistivity, Ground Impedance, and Earth Surface Potentials of a Grounding System," IEEE Std 81, 2012.
[27] O. A. L. De Lima and M. M. Sharma, "A generalized Maxwell-Wagner theory for membrane polarization in shaly sands," *Geophysics*, vol. 57, no. 3, pp. 431–440, 1992.
[28] Z. G. Datsios and P. N. Mikropoulos, "Characterization of the frequency dependence of the electrical properties of sandy soil with variable grain size and water content," *IEEE Trans. Dielectr. Electr. Insul.*, vol. 26, no. 3, pp. 904–912, Jun. 2019.
[29] CIGRE WG C4.33, "Impact of soil-parameter frequency dependence on the response of grounding electrodes and on the lightning performance of electrical systems," Technical Brouchre- 781, 2019.
[30] S. Srinivasan, "Electrode/electrolyte interfaces: structure and kinetics of charge transfer," in *Fuel Cells: From Fundamentals to Applications*, New York, USA: Springer, 2006, pp. 27–92.
[31] F. Batalioto, A. R. Duarte, G. Barbero, and A. M. F. Neto, "Dielectric dispersion of water in the frequency range from 10 mHz to 30 MHz," *J. Phys. Chem.*, vol. 114, pp. 3467–3471, 2010.
[32] A. Revil, "Effective conductivity and permittivity of unsaturated porous materials in the frequency range 1 mHz-1GHz," *Water Resour. Res.*, vol. 49, no. 1, pp. 306–327, 2013.
[33] A. R. Duarte, F. Batalioto, G. Barbero, and A. M. F. Neto, "Electric impedance of a sample of dielectric liquid containing two groups of ions limited by ohmic electrodes: A study with pure water," *J. Phys. Chem. B*, vol. 117, pp. 2985–2991, 2013.
[34] A. R. Duarte, F. Batalioto, G. Barbero, and A. M. Figueiredo Neto, "Measurement of the impedance of aqueous solutions of KCl: An analysis using an extension of the Poisson-Nernst-Planck model," *Appl. Phys. Lett.*, vol. 105, 2014.
[35] H. Hasan, H. Hamzehbahmani, H. Griffiths, D. Guo, and A. Haddad, "Characterization of Site Soils using Variable Frequency and Impulse Voltages," in *Proceedings of 10th Asia -Pacific International Conference on Lightning*, Krabi, Thailand, 2017.
[36] A. Revil *et al.*, "Complex conductivity of soils," *Water Resour. Res.*, vol. 53, no. 8, pp. 7121–7147, 2017.
[37] Z. G. Datsios, P. N. Mikropoulos, and I. Karakousis, "Laboratory measurement of the low-frequency electrical properties of sand," in *Proceedings of 34th ICLP*, Rzeszow, Poland, 2018.
[38] D. P. Lesmes and K. M. Frye, "Influence of pore fluid chemistry on the complex conductivity and induced polarization responses of Berea sandstone," *J. Geophys. Res.*, vol. 106, no. B3, pp. 4079–4090, 2001.
[39] A. R. Miranda, A. Vannucci, and W. M. Pontuschka, "Impedance spectroscopy of water in comparison with high dilutions of lithium chloride," *Mater. Res. Innov.*, vol. 15, no. 5, pp. 302–309, 2011.
[40] S. Srisakot, G. Dana, N. Md Nor, H. Griffiths, and A. Haddad, "Effect of frequency on soil characteristics," 2001.
[41] N. M. Nor, A. Haddad, and H. Griffiths, "Performance of earthing systems of low resistivity soils," *IEEE Trans. Power Deliv.*, vol. 21, no. 4, pp. 2039–2047, Oct. 2006.
[42] J. Montaña, J. Candelo, and O. Duarte, "Sand's electrical parameters vary with frequency," *Ing. e Investig.*, vol. 32, no. 2, pp. 34–39, 2012.
[43] J. He, R. Zeng, and B. Zhang, "Current Field in the Earth," in *Methodology and Technology for Power System Grounding*, 1st ed., Singapore: John Wiley & Sons, 2013, p. 566.
[44] S. Visacro and R. Alipio, "Frequency dependence of soil parameters: Experimental results, predicting formula and influence on the lightning response of grounding electrodes," *IEEE Trans. Power Deliv.*, vol. 27, no. 2, pp. 927–935, 2012.
[45] D. Kuklin, "Device for the field measurements of frequency-dependent soil properties in the frequency range of lightning currents," *Rev. Sci. Instrum.*, vol. 91, no. 11, p. 114701, Nov. 2020,
[46] C. Portela, "Measurements and modeling of soil electromagnetic behavior," in *Proceedings of IEEE International Symposium on Electromagnetic Compatibility*, Seattle, 1999, pp. 1004–1009.
[47] S. Wang *et al.*, "Experimental study on frequency-dependent properties of soil electrical parameters," *Electr. Power Syst. Res.*, vol. 139, pp. 116–120, Oct. 2016, doi: 10.1016/j.epsr.2015.11.018.
[48] M. Zhou, J. Wang, L. Cai, and Y. Fan, "Laboratory investigations on factors affecting soil electrical resistivity and the measurement," *IEEE Trans. Ind. Appl.*, vol. 2015, pp. 5358–5365, 2015.
[49] H. Wakamatsu, "A Dielectric Spectrometer for Liquid Using the Electromagnetic Induction Method," *Hewlett-Packard J.*, pp. 1–10, 1997.
[50] K. Asami, E. Gheorghiu, and T. Yonezawa, "Real-time monitoring of yeast cell division by dielectric spectroscopy," *Biophys. J.*, vol. 76, no. 6, pp. 3345–3348, 1999.
[51] P. Ben Ishai, M. S. Talary, A. Caduff, E. Levy, and Y. Feldman, "Electrode polarization in dielectric measurements: A review," *Meas. Sci. Technol.*, vol. 24, no. 10, 2013.
[52] S. Visacro, R. Alipio, M. H. Murta Vale, and C. Pereira, "The response of grounding electrodes to lightning currents: The effect of frequency-dependent soil resistivity and permittivity," *IEEE Trans. Electromagn. Compat.*, vol. 53, no. 2, pp. 401–406, 2011.
[53] D. Clark *et al.*, "Controlled large-scale tests of practical grounding electrodes - Part II: Comparison of analytical and numerical predictions with experimental results," *IEEE Trans. Power Deliv.*, vol. 29, no. 3, pp. 1240–1248, 2014.
[54] M. Geyab, A. A. Quadir, H. Griffiths, N. Harid, D. Clark, and A. Haddad, "Effect of current magnitude on measured apparent resistance of ground electrodes for 3 and 4-terminal low-voltage test configurations," in *Proceedings of International Conference on Grounding and Earthing & 8th International Conference on Lightning Physics and Effects*, Pirenópolis, Brazil, 2018.
[55] R. Alipio and S. Visacro, "Modeling the frequency dependence of electrical parameters of soil," *IEEE Trans. Electromagn. Compat.*, vol. 56, no. 5, pp. 1163–1171, 2014.
[56] N. Harid, D. Lathi, H. Griffiths, and A. Haddad, "Characterization of ground electrodes under low voltage variable frequency and impulse energization," in *Proceedings of 2015 Asia-Pacific International Conference on Lightning (APL)*, Nogoya, Japan, 2015.
[57] M. C. Hegg and A. V. Mamishev, "Influence of variable plate separation on fringing electric fields in parallel-plate capacitors," in *Conference Record of the 2004 IEEE International Symposium on Electrical Insulation*, 2004, pp. 384–387.
[58] H. A. Haus and J. R. Melcher, *Electromagnetic fields and energy*. Prentice Hall, 1989.
[59] L. A. Geddes and R. Roeder, "Measurement of the direct-current (Faradic) resistance of the electrode-electrolyte interface for commonly used electrode materials," *Ann. Biomed. Eng.*, vol. 29, no. 2, pp. 181–186, 2001.
[60] D. Fortuné, D. Istrate, F. Ziadé, and I. Blanc, "Measurement method of AC current up to 1 MHz," in *20th IMEKO TC4 International Symposium, Benevento*, 2014, pp. 35–39.